Abrasion-set limits on Himalayan gravel flux

Citation for published version:
Dingle, E, Attal, M & Sinclair, H 2017, 'Abrasion-set limits on Himalayan gravel flux', *Nature*, vol. 544, pp. 471–474. https://doi.org/10.1038/nature22039

Digital Object Identifier (DOI):
10.1038/nature22039

Published In:
Nature

Abrasion-set limits on Himalayan gravel flux

Authors: Elizabeth H. Dingle[1*], Mikaël Attal[1], Hugh D. Sinclair[1]

Affiliations:

[1] School of GeoSciences, University of Edinburgh, Drummond Street, Edinburgh EH8 9XP, UK.

*Correspondence to: elizabeth.dingle@ed.ac.uk

Summary: **Rivers sourced in the Himalaya carry some of the largest sediment loads on the planet[1], yet coarse gravel in these rivers vanishes within approximately 20-40 kilometres on entering the Ganga Plain. Understanding where the gravel goes is crucial to forecasting the response of rivers to large pulses of sediment triggered by earthquakes and storms. Rapid increase in gravel flux and subsequent channel bed aggradation following the 1999 Chi-Chi and 2008 Wenchuan earthquakes[2-7] reduced channel capacity and increased flood inundation[3]. Through an analysis of fan geometry, sediment grain size and lithology, we demonstrate that gravel flux from rivers draining the central Himalaya with contributing areas spanning three orders of magnitude is approximately constant. Our findings show that abrasion of gravel during fluvial transport can explain this observation; most of the gravel sourced from more than 100 km upstream is converted into sand by the time it reaches the Plain. These results indicate that earthquake-induced sediment pulses sourced from the Greater Himalaya, such as following the 2015 Gorkha earthquake[8], are unlikely to drive increased gravel aggradation at the mountain front. Instead, they should result in**

an elevated sand flux, leading to distinct patterns of aggradation and flood risk in the densely populated, low-relief Ganga Plain.

Numerical models of foreland basin stratigraphy and modern river systems suggest that the location where river bed sediment texture changes from gravel to sand-dominated (the gravel-sand transition) is determined by: 1) basin subsidence rate; 2) total sediment flux; 3) gravel-size fraction, and 4) river discharge, over sub-millennial timescales[9-13]. However, few field data have previously been available to validate such models. The gravel-sand transition is marked by an abrupt decrease in grain size[14-16], believed to result from an exhaustion of gravel supply. The gravel-sand transition in large trans-Himalayan rivers feeding the Ganga Plain occurs at ~12-20 km downstream of the mountain front in the east Ganga Plain, and slightly further at ~28-45 km in the west Ganga Plain (Fig. 1); this transition is also associated with a marked decrease in channel gradient[17]. We find that the gravel-sand transition in rivers draining small foothill-fed catchments (<350 km^2) in the east Ganga Plain[16] is at a comparable distance downstream of the mountain front to the adjacent trans-Himalayan Gandak and Kosi rivers (>30,000 km^2) (Fig. 1). While spatial variations in basin subsidence across the entire foreland basin may control the overall position of the gravel-sand transition[9, 17], subsidence can be ruled out as a factor explaining this observation, as there is no evidence for a significant variation in subsidence rate beneath the foothill-fed tributaries flowing in the interfan region between the Gandak and Kosi alluvial fans[17]. Given the substantial contrast in size between the trans-Himalayan Gandak and Kosi rivers and the smaller foothill-fed catchments, we would expect orders of magnitude differences in water and total sediment flux, which is at odds with the similarity in the positions of the gravel-sand transition. These fluxes are therefore also unlikely to play a significant role in controlling the position of this transition. Gravel fining rates between the mountain front and the gravel-sand transition in the east Ganga Plain are also independent of the relatively rapid reduction in grain size observed across the gravel-sand transition[16, 17]. This further indicates that neither abrasion downstream of the mountain front nor input grain size exert a dominant control on the distance to the transition in the Ganga Plain. Theory and experiments have implied that an increase in the fraction of gravel in the sediment supplied to the basin results in progradation of the gravel front[9]. Having ruled out other likely controls, we further test whether the position of the gravel-sand transition across the east Ganga Plain reflects differences (or similarities) in gravel flux.

We first compare the total mass flux of sediment exported into the Plain to the mass trapped upstream of the gravel-sand transition. The volume of gravel between the mountain front and the mapped gravel-sand transitions[17] is calculated using the mean basin subsidence rate (which is believed to have been relatively constant over the last 10^4 years[17]), the distance to the gravel-sand transition, and the maximum width of the alluvial fan (see Methods). We assume that most gravel is trapped upstream of the gravel-sand transition, an assumption supported by the conspicuous lack of gravel downstream of the transition. The use of the basin subsidence rate assumes the degree of filling of accommodation space (defined by a depositional base-level) during that interval is constant (see Extended Data). The gravel-to-total-load ratio was also calculated for each catchment. Total sediment flux data are only available for the trans-Himalayan rivers considered in this study[18], so to approximate total sediment flux from the smaller foothill catchments (Churre, Bakeya, Lakhandei, Ratu, and Aurhi), we have used ^{10}Be-derived catchment-averaged erosion rates from similar sized catchments further west in the Garhwal Himalaya[19] (see Methods).

We find that absolute gravel fluxes are lower across the foothill catchments, with values typically ranging between 0.05 and 0.72 Mt/yr, compared to values of 0.51-3.29 Mt/yr in the trans-Himalayan catchments, but the differences are significantly smaller than what would be expected from catchments with contributing areas spanning three orders of magnitude (Fig. 2a). These absolute flux values should be treated as a maximum however, as we assume that that the full surface of the fan is available to receive sediment (see Methods). Our gravel proportion (or gravel-to-total-load ratio) estimates for the large trans-Himalayan systems vary between 0.2 and 29%, with proportions generally lowest for the Gandak and Kosi rivers in the east Ganga Plains (Fig. 2b). For average and maximum sediment flux scenarios (using average and maximum erosion rates), gravel proportions are systematically lower than estimates based on a similar abrasion model to predict gravel proportion for major Himalayan rivers at the mountain front[20]. For the smaller foothill catchments, gravel proportions are notably higher, even under the maximum flux scenario with catchment-averaged erosion rates of 5 mm/yr (Fig. 2b); for the gravel proportion to be lower than 50%, larger total sediment fluxes would be required, suggesting catchment-averaged erosion rates in excess of ~2.75 mm/yr.

Identification of the provenance of gravel is facilitated by the fact that the Himalayan mountain range is divided into four major structural units that run broadly parallel from west to east and are composed of contrasted lithological units (Fig. 1). These units are from north to south: the Tethyan Himalayan Sequence, the Greater Himalayan metamorphic unit, the Lesser Himalayan Sequence and the Siwalik Group[21] (see Methods). The Main Frontal Thrust is the most southerly tectonic structure, situated between the Siwalik Group and the foreland basin, and absorbs approximately 80% of the ~21±1.5 mm/yr convergence between India and south Tibet[22]. During the low-flow season (October-May), a considerable portion of the channel bed of major rivers of the Ganga basin is accessible, with extensive coarse gravel bars dominating the bed of the rivers as they cross the mountain front. To assess gravel provenance, pebble lithology was identified at a number of sites from ~30 to 50 km upstream of the mountain front down to the gravel-sand transition in each of the trans-Himalayan rivers (Fig. 1). Using a 25 m tape measure, pebble lithology was identified at 50 cm intervals along two transects at each site and categorised as outlined in Methods.

Clast characterisation shows that gravel which could be identified as uniquely from the Tethyan Himalayan sedimentary lithologies was absent from all our sites (see Methods), despite this unit representing 10-20% of the total catchment geology (Fig. 3a and Extended Data Figure 1). Quartzites are considered separately as they are distributed within each of the contributing units but cannot be traced back to any specific one. Quartzites represent a small fraction of the rocks exposed in the catchments, typically less than 10%[20], yet they constitute the majority of the pebbles sampled (~40-70%), consistent with observations along the Marsyandi River[20]. Lesser Himalayan metamorphic lithologies comprised ~5-40% of sampled pebbles (Fig. 3b). In general, where Lesser Himalayan lithologies covered a larger proportion of the total catchment area (such as for the Yamuna), a higher proportion of Lesser Himalayan lithologies was found in the sampled pebbles (Fig. 3b). Greater Himalayan lithologies (igneous and medium to high grade metamorphic) comprised a further 5-40 % of the sampled pebbles, with the greatest proportions found further east along the Gandak and Kosi rivers where the Greater Himalayan source rocks extend further south. Sedimentary Siwalik lithologies made up a relatively small fraction (<10%) of the sampled pebbles.

For our numerical model experiments, we used three pebble erodibility coefficients typical of the Himalayan lithologies[23] to assess the likelihood for gravel supplied from different parts of the catchments to survive as gravel after transportation to the mountain front. Using published percent mass loss per travelled distance values[23], we explored model scenarios on the Kosi and Bakeya catchments to define how pebble erodibility influences the proportion of the catchment area contributing gravel to the Plain as a function of catchment size[23,24] (see Methods).

Modelling results show that for weak lithologies with high erodibility values (λ) such as schist and poorly cemented sandstones[23], only locally sourced gravel is likely to survive at the mountain outlet (Fig. 4). After a transport distance of ~20 km, most gravel with high erodibility (λ = 20 %/km) is abraded and converted into sand and finer products[23]; therefore, most of the easily erodible gravel supplied to the river at a distance greater than ~20 km upstream of the mountain front is unlikely to contribute to the gravel load, and is likely transported as washload or suspended load. Gravel with erodibility values of around 2 %/km, representative of most Himalayan lithologies such as gneiss, granite, limestone and well-cemented sandstone, can survive transport lengths of ~100-200 km. Clasts of these lithologies would likely constitute a greater proportion of gravel material at the outlet; this however is a conservative estimate, as chemical weathering on hillslopes and during temporary storage may weaken pebbles[25]. Under the lowest erodibility values (λ = 0.2 %/km, e.g. quartzite[23]), a large proportion of the gravel supplied to the rivers is likely to survive to the mountain front (Fig. 4).

Modelling of the abrasion of gravel as it is transported downstream suggests that beyond a critical fluvial transport length upstream of the mountain front, gravel delivered to the fluvial network reaches the Ganga Plain mainly as sand and finer sediment[18,23,24] (Fig. 4). This is consistent with Sr-Nd isotopic mass balances of suspended sediment in the Ganga Basin suggesting that 80±10% of suspended sediment delivered to the Plain is of Greater Himalayan source, whilst only 20±10% is sourced from the Lesser Himalaya[26]. The critical fluvial transport length is dependent on pebble erodibility, which is a function of lithology, and was estimated to be in the order of $250/\lambda$ [(23)]. For trans-Himalayan catchments, intermediate and low strength lithologies of the Lesser and Greater Himalaya sourced within ~100 km upstream of the mountain front will contribute a significant fraction of the gravel exported and deposited upstream of the gravel-sand transition[23]. Similar lithologies sourced further upstream will be abraded into sand prior to reaching the outlet, which is supported by the lack of pebbles distinctively sourced from the Tethyan Himalaya and relatively low proportions of Greater Himalayan pebbles in the Plain (Fig. 3). Where Greater Himalayan rocks are exposed further south in these catchments, a larger proportion of Greater Himalayan pebbles reach the Plain as a result of shorter transport distances and generally lower percent mass loss of Greater Himalaya lithologies (e.g. gneiss, granite) via abrasion, compared to the sedimentary and low grade metamorphics from the other contributing units[20, 23]. More resistant quartzite lithologies, however, are sourced from all parts of the Himalaya[20]. Even in catchments as large as the Kosi, more than 50 % of quartzitic pebbles sourced from the catchment headwaters are likely to reach the mountain outlet as gravel, as the characteristic transport length for quartzite (> 1000 km [(23)]) is longer than the river network (Fig. 4). We would therefore expect quartzite to dominate the lithologies of pebbles exported into the Plain, which is consistent with our observations (Fig. 3b) and with previous modelling predicitions[23, 24]. The smaller foothill catchments are draining the Neogene Siwalik sediments which consist of previously deposited Plain sediments which are progressively incorporated back into the mountain range through frontal accretion of thrust units[16]. Therefore, the rivers are expected to recycle almost exclusively quartzitic gravel, which is confirmed by field observations. The low degree of cementation of the young Neogene sediment was also noted in the field, which likely explains the high catchment-averaged erosion rates. These observations explain why a very high proportion of the gravel delivered to the foothill channels survive into the Plain, and hence, why high gravel fluxes per unit catchment area are observed for these smaller systems (Fig. 2a).

Our models and data demonstrate that increased sediment delivery to channels will result in an additional pulse of gravel reaching the Plain only if sediment delivery occurs within less than ~100 km upstream of the mountain front or is sourced in highly resistant lithologies (e.g. quartzite). Increased gravel supply to rivers in the Siwalik Hills (proximal and quartzite-dominated), such as might be expected from landsliding following seismicity on the Main Frontal Thrust, will likely result in a pulse of gravel and aggradation in river channels of the proximal Plain. Conversely, widespread landsliding in the Greater Himalaya[8] initiated by the 2015 Gorkha earthquake (>200 km upstream of the mountain outlets) should result in elevated sand flux but is less likely to drive increased gravel flux to the Plain and thus leave a trace in the gravel stratigraphy of the foreland basin (see Extended Data Figure 3). Our results also suggest that over the length scale of trans-Himalayan rivers, abrasion facilitates the downstream translation and dispersion of earthquake generated sediment[27] through the transformation of gravel to more mobile sand. The 1950 Assam earthquake reportedly dislodged 47 billion m^3 of landslide material[28], resulting in a long-term channel aggradation and morphological change in tributaries of the Brahmaputra River[29], although the relative effects of increased gravel and sand delivery out of the mountain front were not explored. Rivers in the Plain are expected to respond differently to elevated sand or gravel input; our findings suggest that understanding these contrasted responses represents a timely avenue for future research.

References:

1. Milliman, J. D. & Syvitski, J. P. M. Geomorphic/Tectonic Control of Sediment Discharge to the Ocean: The Importance of Small Mountainous Rivers. *The Journal of Geology* **100,** 525–544 (1992).
2. Dadson, S. J. *et al.* Earthquake-triggered increase in sediment delivery from an active mountain belt. *Geology* **32,** 733–736 (2004).
3. Chen, H. & Petley, D. N. The impact of landslides and debris flows triggered by Typhoon Mindulle in Taiwan. *Quarterly Journal of Engineering Geology and Hydrogeology* **38,** 301–304 (2005).
4. Yanites, B. J., Tucker, G. E., Mueller, K. J. & Chen, Y.-G. How rivers react to large earthquakes: Evidence from central Taiwan. *Geology* **38,** 639–642 (2010).
5. Dadson, S. J. *et al.* Links between erosion, runoff variability and seismicity in the Taiwan orogen. *Nature* **426,** 648–651 (2003).
6. Huang, R. & Fan, X. The landslide story. *Nature Geosci* **6,** 325–326 (2013).
7. Yanites, B. J. *et al.* The influence of sediment cover variability on long-term river incision rates: An example from the Peikang River, central Taiwan. *J. Geophys. Res.* **116,** F03016 (2011).

8. Kargel, J. S. *et al.* Geomorphic and geologic controls of geohazards induced by Nepal's 2015 Gorkha earthquake. *Science* **351,** aac8353 (2016).

9. Paola, C., Heller, P. L. & Angevine, C. L. The large-scale dynamics of grain-size variation in alluvial basins, 1: Theory. *Basin Research* **4,** 73–90 (1992).

10. Parker, G. & Cui, Y. The arrested gravel front: stable gravel-sand transitions in rivers Part 1: Simplified analytical solution. *Journal of Hydraulic Research* **36,** 75–100 (1998).

11. Robinson, R. A. J. & Slingerland, R. L. Origin of Fluvial Grain-Size Trends in a Foreland Basin: The Pocono Formation on the Central Appalachian Basin. *Journal of Sedimentary Research* **68,** (1998).

12. Hoey, T. B. & Bluck, B. J. Identifying the Controls Over Downstream Fining of River Gravels. *Journal of Sedimentary Research* **69,** (1999).

13. Marr, J. G., Swenson, J. B., Paola, C. & Voller, V. R. A two-diffusion model of fluvial stratigraphy in closed depositional basins. *Basin Research* **12,** 381–398 (2000).

14. Ferguson, R., Hoey, T., Wathen, S. & Werritty, A. Field evidence for rapid downstream fining of river gravels through selective transport. *Geology* **24,** 179–182 (1996).

15. Ferguson, R. I. Emergence of abrupt gravel to sand transitions along rivers through sorting processes. *Geology* **31,** 159–162 (2003).

16. Dubille, M. & Lavé, J. Rapid grain size coarsening at sandstone/conglomerate transition: similar expression in Himalayan modern rivers and Pliocene molasse deposits. *Basin Res* **27,** 26–42 (2015).

17. Dingle, E. H., Sinclair, H. D., Attal, M., Milodowski, D. T. & Singh, V. Subsidence control on river morphology and grain size in the Ganga Plain. *Am J Sci* **316,** 778–812 (2016).

18. Lupker, M. *et al.* 10Be-derived Himalayan denudation rates and sediment budgets in the Ganga basin. *Earth and Planetary Science Letters* **333–334,** 146–156 (2012).

19. Scherler, D., Bookhagen, B. & Strecker, M. R. Tectonic control on 10Be-derived erosion rates in the Garhwal Himalaya, India. *J. Geophys. Res. Earth Surf.* **119,** 2013JF002955 (2014).

20. Attal, M. & Lavé, J. Changes of bedload characteristics along the Marsyandi River (central Nepal): Implications for understanding hillslope sediment supply, sediment load evolution along fluvial networks, and denudation in active orogenic belts. *Tectonics, Climate and Landscape Evolution: Geological Society of America Special Paper 398* 143–171 (2006).

21. Yin, A. Cenozoic tectonic evolution of the Himalayan orogen as constrained by along-strike variation of structural geometry, exhumation history, and foreland sedimentation. *Earth-Science Reviews* **76,** 1–131 (2006).

22. Lavé, J. & Avouac, J. P. Active folding of fluvial terraces across the Siwaliks Hills, Himalayas of central Nepal. *Journal of Geophysical Research: Solid Earth* **105,** 5735–5770 (2000).

23. Attal, M. & Lavé, J. Pebble abrasion during fluvial transport: Experimental results and implications for the evolution of the sediment load along rivers. *J. Geophys. Res.* **114,** F04023 (2009).

24. Sklar, L. S., Dietrich, W. E., Foufoula-Georgiou, E., Lashermes, B. & Bellugi, D. Do gravel bed river size distributions record channel network structure? *Water Resour. Res.* **42,** W06D18 (2006).

25. Heller, P. L. *et al.* Paradox of downstream fining and weathering-rind formation in the lower Hoh River, Olympic Peninsula, Washington. *Geology* **29**, 971-974 (2001).

26. Galy, A. & France-Lanord, C. Higher erosion rates in the Himalaya: Geochemical constraints on riverine fluxes. *Geology* **29,** 23–26 (2001).

27. Cui, Y. *et al.* Sediment pulses in mountain rivers: 1. Experiments. *Water Resour. Res.* **39,** 1239 (2003).

28. Keefer, D. K. Earthquake-Induced Landslides and Their Effects on Alluvial Fans. *Journal of Sedimentary Research* **69,** (1999).

29. Sarma, J. N. Fluvial process and morphology of the Brahmaputra River in Assam, India. *Geomorphology* **70,** 226–256 (2005).

Acknowledgments: We thank V. Singh, A. Gajurel, J. Stewart, F. Bowyer, K. Maheswari, D. Basuroy, A. Sarkar, B. Sitaula and Apex Adventure, and the Nepalese Department of Mines and Geology for their cooperation and logistical support in the field. E. Garzanti and two anonymous reviewers provided thoughtful and constructive comments that have greatly helped to improve this manuscript. We are also grateful to the International Association of Sedimentologists, British Society for Geomorphology and the Edinburgh University Club of Toronto for their financial support of the fieldwork. This study formed part of a Natural Environment Research Council (NERC) funded PhD (NE/L501566/1). All data presented are available in the manuscript and accompanying documents (Methods, Extended Data).

Author Contributions: E.H.D. and M.A. collected pebble lithology data and mapped positions of the gravel-sand transition. E.H.D. calculated gravel fluxes and proportions. M.A. devised the pebble abrasion model, which E.H.D. ran and analysed the results from. E.H.D., M.A. and

H.D.S. designed the study and all discussed the results to shape this manuscript. E.H.D. M.A. and H.D.S wrote the manuscript. Figures were produced by E.H.D.

Author information: Reprints and permissions information is available at www.nature.com/reprints. The authors declare no competing financial interests. Correspondence and requests for materials should be addressed to E.H.D. (elizabeth.dingle@ed.ac.uk).

Figure 1 | Study area and simplified geological map of the Ganga basin. The mapped gravel-sand transition is shown for both the major trans-Himalayan rivers[17] and smaller foothill-fed catchments[16] considered in the east Ganga Plain. Major geological units[21] are all bound by major faults. The red dashed line links the position of mapped gravel-sand transitions between rivers in the Plain.

Figure 2 | Gravel flux estimates. a, Absolute gravel flux estimates (black) and gravel flux per unit catchment area (red) estimates for trans-Himalayan and foothill-fed (shaded in grey) rivers. **b,** Calculated percent gravel exported by trans-Himalayan rivers into the Ganga Plain (see Methods and Extended Data). Foothill-fed catchments are shaded in grey. Red, blue and yellow data points correspond to maximum, average and minimum total sediment flux scenarios, respectively, with corresponding erosion rates (in mm/yr) indicated next to data points for maximum and minimum flux scenarios for reference. Error bars in subplots reflect differences in accommodation space generated under maximum and minimum subsidence rates[17].

Figure 3 | Catchment and pebble lithology. a, Proportion of area of major geological units in trans-Himalayan catchments upstream of the mountain front[21]. **b,** Average clast lithology composition recorded on exposed gravel bars between the mountain front and the gravel-sand transition (see Extended Data Figure 1 for pebble lithology at each survey location). Quartzites are considered separately as they are distributed within each of the contributing units but cannot be traced back to any of these units; they represent a small fraction of the rocks exposed in the catchments, typically less than 10%[20].

Figure 4 | Abrasion scenarios for the Kosi (top - trans-Himalayan) and Bakeya (bottom – foothill-fed) rivers. Three pebble erodibility values are used, representative of Himalayan lithologies[20, 23]. Colour indicates the percentage of gravel supplied to the river at this location that reaches the catchment outlet as gravel; the remaining percentage represents the mass loss by abrasion, assumed in this case to be sand and finer sediment. More than 50 % of the gravel supplied by pixels in dark blue reaches the outlet as gravel; almost all of the gravel supplied by pixels in pale lilac is turned into sand and finer products before reaching the outlet.

Methods:

Gravel flux estimates

The volume of accommodation space generated between the mountain front and mapped gravel-sand transition was calculated for each catchment to estimate the volume of gravel trapped upstream of the gravel-sand transition. The volume generated each year was defined as the product of basin subsidence rate[17], distance to the gravel-sand transition, and maximum width of the alluvial fan upstream of the transition derived from Google Earth imagery. The gravel-sand transition was mapped for each river by noting the point at which exposed deposits were nearly exclusively sand (> 95%) [17].

The lateral extent of alluvial fans was determined by topographic barriers, or where fans from adjacent systems constrain lateral mobility[30]. Where closely spaced, similar sized channels exit the mountain front and it was difficult to constrain fan boundaries, the maximum width of each fan was set as the mid-point between the two channel outlets. This area represents the maximum extent over which the channel can deposit sediment upstream of the gravel-sand transition. We assume that deposition will occur over the total surface of this area over timescales of 10^1-10^3 years, based on documented avulsion pathways on the Kosi River which appear to inundate the surface of the Kosi mega-fan upstream of the gravel-sand transition over ~200 years[31], and for consistency with ^{10}Be derived sediment fluxes that are averaged over 10^2-10^3 years[18]. Whilst the modern channel only occupies a portion of the fan surface, repetitive phases of channel infilling and avulsion over these timescales allow the channel to migrate over the surface of the fan making the entire fan surface available to receive sediment[31]. We also assume that the distance from the mountain front to the gravel-sand transition remains relatively constant over these timescales, which is supported by the presence of a channel slope break at the transition. A translation of this transition a few km downstream or upstream would not significantly affect the gravel proportion estimates. This is demonstrated in Extended Data Figure 2, where gravel proportions have been recalculated based on the gravel-sand transition being 5 km further upstream or downstream. The total available accommodation space upstream of the gravel-sand transition was converted to a total mass of sediment, assuming densities typical of quartzite (2.65 t/m^3). The mass of coarse sediment trapped upstream of the gravel-sand transition was then converted to a proportion of the total sediment flux (see Extended Data).

Foothill-fed catchment sediment fluxes

Where sediment flux data are not available for the foothill-fed catchments (Churre, Bakeya, Lakhandei, Ratu, and Aurhi), ^{10}Be-derived catchment-averaged erosion rates from similar sized catchments further west in the Garhwal Himalaya[19] have been used to approximate total sediment fluxes. These sub-catchments form part of the Yamuna catchment, but are higher in elevation and catchment relief than the foothill-fed catchment considered in this study, with average elevations between ~1700- 4000 m. With this in mind, we have calculated sediment fluxes for the foothill catchments using the maximum range of erosion rates reported from these data (0.5 – 5 mm/yr), and assuming an average rock density of 2.65 t/m^3.

Bedload is commonly assumed to constitute ~10% of total river sediment loads in rivers originating from mountainous settings, although this proportion decreases to as low as 1% with increasing catchment areas above ~10^3 km^2 [(32)]. Our gravel flux estimates should represent a minimum bedload flux as they do not incorporate sediment finer than 2 mm which may also be transported as bedload. Our gravel proportion estimates (and gravel flux per unit catchment area) appear much larger in small foothill-fed systems than in trans-Himalayan catchments. To generate total sediment fluxes large enough to allow gravel proportions in keeping within these empirical relationships[32], catchment averaged erosion rates of 3-5 mm/yr are required in the foothill catchments. Either these catchments experience relatively high erosion rates (comparable to the fastest eroding catchments further west in the Garhwal Himalaya[19]), or gravel makes up a larger proportion of the total sediment load (>50 %) than might be expected based on an empirically derived catchment area scaling relationship[32]. Conversely, gravel proportions in the larger trans-Himalayan systems are low, representing as little as ≤1 % of the total sediment load (Fig. 2b). This could be a result of over-estimated ^{10}Be-derived erosion rates.

Influence of abrasion on spatial distribution of sources of gravel

We applied a simple abrasion model to produce Figure 4. Using a 30 m Shuttle Radar Topography Mission (SRTM) Digital Elevation Model (DEM), we calculated the distance α between each contributing pixel and the catchment outlet and used Sternberg's law to calculate the proportion K of the gravel initially supplied by the pixel that reaches the catchment outlet as gravel[20, 23]:

$$K = e^{-\lambda\alpha} \qquad (1)$$

where λ is the percent gravel (or pebble) mass loss per km and $K = M/M_0$, where M_0 represents the mass of gravel initially supplied by the pixel and M the remaining mass of gravel after a transport distance α. We assume that all products of abrasion are sand and finer sediment[23]. We made the calculation for three erodibility coefficients representative of Himalayan lithologies for both a trans-Himalayan catchment (Kosi River, maximum stream length ~600 km, drainage area ~50,000 km^2) and a foothill catchment (Bakeya River, maximum stream length ~50 km, drainage area ~350 km). Maps were generated with constant erodibility coefficients across the whole catchments for illustrative purpose (Figure 4), using coefficients of 0.2, 2 and 20 percent mass loss per km, representative of the hardest, most common, and weakest lithologies exposed in the catchments, respectively[20, 23]. We note that spatial variations in erosion rates could affect the absolute gravel flux supplied from different parts of the catchment and therefore the relative proportions of a given lithology on gravel bars. For example, higher erosion rates are expected in areas supplying Greater Himalaya lithologies[20, 22], which should lead to a relatively higher abundance of gravel from these lithologies compared to a scenario with uniform erosion; however, this does not affect the maps shown in Figure 4 as they relate the fraction of gravel remaining after transport to the outlet to the fraction of gravel initially supplied by a given pixel, irrelevant of the absolute volume (or flux) supplied. Similarly, some lithologies may contribute a relatively greater amount of gravel than others[20] but again this does not affect the maps shown in Figure 4.

Determination of pebble lithology in the field

The four major structural units running broadly parallel from west to east across the Himalayan orogen are from north to south: the Tethyan Himalayan Sequence, the Greater Himalayan metamorphic unit, the Lesser Himalayan Sequence and the Siwalik Group[21, 33]. The Tethyan Sequence contains marine sedimentary to low grade meta-sedimentary rocks. The Greater Himalayan metamorphic unit consists largely of medium to high grade schist, paragneiss and orthogneiss[34]. The Lesser Himalayan Sequence comprises lower grade metasedimentary rocks including phyllite, quartzite, marble and dolostone[21, 34]. The Siwalik Group contains Neogene sandstones, conglomerates and shales, formed by the erosional products of the Lesser and Greater Himalaya[35].

Between six and eleven gravel bars located between up to ~100 km upstream of the mountain front and the gravel-sand transition were surveyed along each river. At each site, two 25 m long lines were positioned near the center of the bar, parallel to the river, and the lithology of each pebble was recorded every 0.5 m [(20)]. The percentage lithology numbers obtained from this survey are directly comparable to volumetric proportions, with surface and sub-surface samples typically yielding comparable results[20]. In terms of lithological identification, quartzite is sourced from all across the Himalaya and, as such, it is not possible to distinguish the quartzite pebble source region from visual inspection. Therefore, quartzite pebbles were grouped into a separate lithology category. Low to medium grade metamorphic rocks were grouped as Lesser Himalayan, whilst medium to high grade metamorphic and igneous rocks were grouped as Greater Himalayan. No pebble that could distinctively be related to the Tethyan Himalayan lithologies was found, though some quartzite pebbles are likely to be sourced from this unit. Similarly, limestone, dolostone or even very low grade metasedimentary clasts may derive from either Tethyan or Lesser Himalayan successions. Siwalik lithologies included Neogene non-metamorphosed sedimentary rocks such as sandstone, mudstones and conglomerates that were easily distinguishable in the field. Proportions of the different lithologies at each site are shown in Extended Data Figure 1. Only the sites downstream of the mountain front were used to produce the data in Figure 3b.

References

30. Leier, A. L., DeCelles, P. G. & Pelletier, J. D. Mountains, monsoons, and megafans. *Geology* **33,** 289–292 (2005).

31. Chakraborty, T., Kar, R., Ghosh, P. & Basu, S. Kosi megafan: Historical records, geomorphology and the recent avulsion of the Kosi River. *Quaternary International* **227,** 143–160 (2010).

32. Turowski, J. M., Rickenmann, D. & Dadson, S. J. The partitioning of the total sediment load of a river into suspended load and bedload: a review of empirical data. *Sedimentology* **57,** 1126–1146 (2010).

33. Gansser A. 1964. The Geology of the Himalayas. *New York: Wiley Interscience*. 289 pp.

34. DeCelles, P. G. *et al.* Neogene foreland basin deposits, erosional unroofing, and the kinematic history of the Himalayan fold-thrust belt, western Nepal. *Geological Society of America Bulletin* **110,** 2–21 (1998).

35. Kumar, R., Sangode, S. J. & Ghosh, S. K. A multistorey sandstone complex in the Himalayan Foreland Basin, NW Himalaya, India. *Journal of Asian Earth Sciences* **23,** 407–426 (2004).

36. Narula, P. L., Acharyya, S. K. & Banerjee, J. Seismotectonic Atlas of India and its Environs: *Calcutta, The Geological Survey of India*. (2000).

37. Sinclair, H. D. & Naylor, M. Foreland basin subsidence driven by topographic growth versus plate subduction. *Geological Society of America Bulletin* **124,** 368–379 (2012).

Data Availability Statement: All data used in the production of this paper and figures are listed in the text or Extended Data. Data presented in Figure 2 were generated using the values listed in Extended Data Tables 1-3 and as discussed in Methods.

Extended Data Figure 1 | Details of pebble lithologies documented on exposed gravel bars along trans-Himalayan rivers upstream of the gravel-sand transition. Data in Figure 3b represent an average of the sites downstream of the mountain front for each river. Note that Siwalik lithologies were found on bars sampled along the Kosi River, despite no Siwalik units being mapped in the catchment geology[21]; this is likely due to the coarse nature of the Himalayan scale geological map[21], where small outcrops may have been omitted.

Extended Data Figure 2 | Sensitivity of gravel proportions to the position of the gravel-sand transition. In this figure, gravel proportions were calculated for instances where the gravel-sand transition was 5 km further downstream and upstream of the mapped position to test the effect on results presented in Figure 2b; these changes are reflected by the increased length of error bars associated with each river, but the overall patterns remain unchanged. As in Figure 2b, gravel percentage values are estimated by dividing the flux of gravel calculated based on fan geometry and location of the gravel-sand transition by the total sediment flux from (i) catchment-averaged ^{10}Be derived erosion rates for trans-Himalayan catchments[18], and (ii) a range of possible catchment-averaged erosion rates for the foothill-fed catchments[19]. Foothill-fed catchments are shaded in grey. Red, blue and yellow data points correspond to maximum, average and minimum total sediment flux scenarios, respectively, with corresponding erosion rates (in mm/yr) indicated next to data points for maximum and minimum flux scenarios for reference. Error bars reflect differences in accommodation space generated under maximum and minimum subsidence rates[17].

Extended Data Figure 3 | Schematic of gravel abrasion and sediment pulse delivery from the interior of the Himalaya into the Ganga Plain. Schematic comparison of the evolution of coarse sediment pulses generated in the Greater Himalaya and Siwalik Hills, as a result of earthquake-induced landsliding. The magnitude and extent of the pulses as they travel downstream is unknown, as is the timescales over which the pulses migrate[27]. **a**, As the sediment pulse is translated and dispersed downstream[27], a combination of abrasion of weaker lithologies sourced in the Higher Himalaya and greater transport distances minimizes the gravel flux reaching the Ganga Plain, downstream of the mountain front. **b**, In contrast, stronger quartzite pebbles sourced from the Siwalik Hills undergo much less abrasion and, when combined with shorter transport distances, a larger gravel flux survives into the Ganga Plain when landsliding is focused closer to the mountain front. A large fraction of this gravel will likely remain trapped upstream of the gravel-sand transition, whereas more mobile sand and finer sediment (generated by the landslide inputs themselves and from the abrasion of coarser sediments) can be transported and deposited further downstream; where and when this finer sediment is deposited between the mountain front and the tip of the Bengal fan is less well understood. **c**, Where gravel flux downstream of the mountain front is enhanced, gravel aggradation could reduce channel capacity and enhance over-bank flooding. The extent of flooding is exacerbated by low-relief topography which characterize sedimentary basins downstream of large mountain ranges.

Extended Data Table 1 | Subsidence and fan geometries used to calculate gravel flux. Data used to calculate gravel fluxes for each catchment. Catchment areas are derived from a 90 m SRTM DEM, whilst distances to the gravel-sand transition are taken from previously published works[16, 17]. Fan widths were determined as outlined in Methods. Maximum, average and minimum total (tectonic plus sediment-load induced) subsidence rates beneath the mountain front were taken from published works[17], based on depth to basement data derived from seismic surveys[36], and horizontal shortening rates between the Ganga Plain and Himalaya. Given the short distances to the gravel-sand transition relative to the full width of the flexural profile that defines the basin, we do not expect a significant decrease in subsidence rate downstream over the lengths considered[37] and as such have not incorporated it into our calculations.

Extended Data Table 2 | Subsidence and fan geometries used to calculate gravel flux. The accommodation space created per year represents the product of the fan width, distance between mountain front and gravel-sand transition, and subsidence rate. These accommodation space values should be considered as a maximum, given that we assume that subsidence rate does not decrease with distance downstream of the mountain front, and that the entire surface of the fan is available to receive sediments (see Methods). Minimum, average and maximum gravel fluxes (Mt/yr) are calculated by multiplying the accommodation space generated by a density of 2.65 t/m^3 reflecting the quartzite and quartz sand (~15%)[17] nature of sediments trapped upstream of the gravel-sand transition.

Extended Data Table 3 | Sediment fluxes and gravel ratios. Sediment fluxes, catchment-averaged erosion rates and gravel-to-total-sediment-load proportions. Gravel-to-total-sediment-load proportions were calculated using the gravel fluxes shown in Extended Data Table 2 and total sediment fluxes below from literature[17, 18]. The maximum gravel proportion here reflects the scenario with the lowest total sediment flux and highest subsidence rate/maximum accommodation space. Conversely, the minimum gravel proportion represents the scenario with the highest sediment flux and lowest subsidence rate/minimum accommodation space.

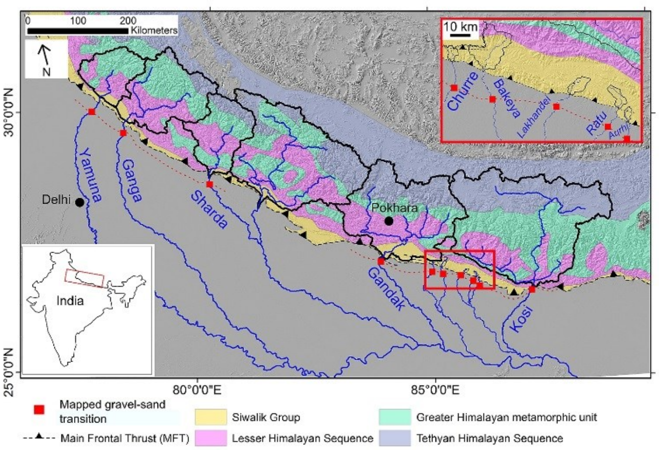

0 100 200 Kilometers
N
10 km
Churre
Bakeya
Lakhandei
Ratu
Aurhi
30°0'0"N
25°0'0"N
80°0'0"E
85°0'0"E
Yamuna
Ganga
Sharda
Delhi
Pokhara
Gandak
Kosi
India
Mapped gravel-sand transition
Main Frontal Thrust (MFT)
Siwalik Group
Lesser Himalayan Sequence
Greater Himalayan metamorphic unit
Tethyan Himalayan Sequence

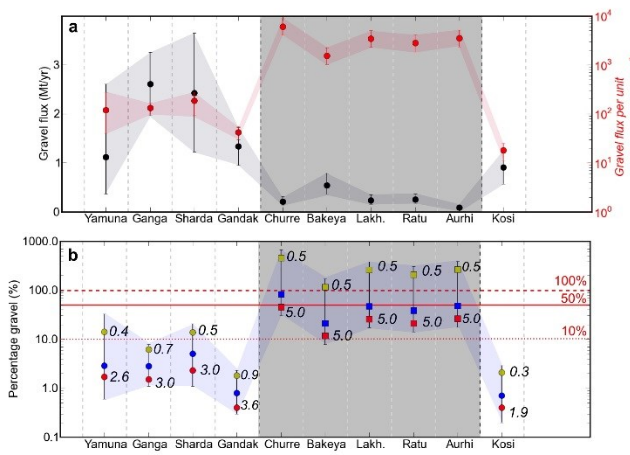
a
b
Gravel flux (Mt/yr)
Gravel flux per unit catchment area (t/km²)
Percentage gravel (%)
Yamuna
Ganga
Sharda
Gandak
Churre
Bakeya
Lakh.
Ratu
Aurhi
Kosi
100%
50%
10%
0.4
2.6
0.7
3.0
0.5
3.0
0.9
3.6
0.5
5.0
0.5
5.0
0.5
5.0
0.5
5.0
0.5
5.0
0.3
1.9

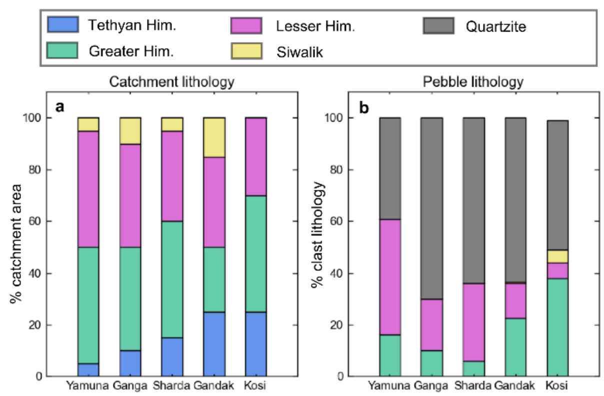
Tethyan Him.
Greater Him.
Lesser Him.
Siwalik
Quartzite
Catchment lithology
a
% catchment area
Yamuna Ganga Sharda Gandak Kosi
Pebble lithology
b
% clast lithology
Yamuna Ganga Sharda Gandak Kosi

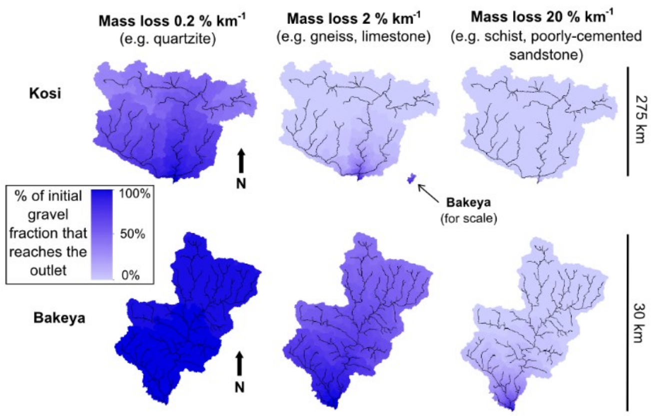

Mass loss 0.2 % km^{-1}
(e.g. quartzite)
Mass loss 2 % km^{-1}
(e.g. gneiss, limestone)
Mass loss 20 % km^{-1}
(e.g. schist, poorly-cemented sandstone)
Kosi
275 km
N
% of initial gravel fraction that reaches the outlet
100%
50%
0%
Bakeya
(for scale)
Bakeya
30 km
N